Hydrography in the north-western Barents Sea, July–August 1996

Terje Brinck Løyning

CTD profiles from the north-western Barents Sea, sampled in July–August 1996, have been analysed and characteristics of water masses have been compared with former analyses and investigations. The barotropic and baroclinic modes of the Rossby radius of deformation have been estimated in order to give an estimate of the spatial scale of variations. The first baroclinic mode of the Rossby radius of deformation is estimated to be around 3 km. Cold halocline water (CHW) is found in the southern part of the investigation area, supporting a hypothesis that the production of CHW is located in the area around Storbanken, and not closer to the shelf break further north. Another hypothesis is proposed: tidal induced horizontal circulation and vertical currents may explain a northward transport of warmer water across sills and banks in the north-western Barents Sea.

T. B. Løyning, Norwegian Polar Institute, Polar Environmental Centre, N-9296 Tromsø, Norway.

As described by several authors the last century, the source of heat and salt to the Barents Sea is the North Atlantic Current (NAC) (Helland-Hansen & Nansen 1909; Loeng 1991; Pfirman et al. 1994; Steele et al. 1995; Harris et al. 1998). Most of these studies have focused on the area between Norway and Spitsbergen, i.e. the south-western parts of the Barents Sea, where the NAC splits in two branches. One branch continues northwards along the continental slopes as the West Spitsbergen Current, and the other flows into the Barents Sea along the Bjørnøyrenna (Bear Island Trough). Several studies indicate that the currents are topographically steered (Rudels 1987; Johansen et al. 1988; Loeng 1990, 1991; Pfirman et al. 1994; Gawarkiewicz & Plueddemann 1995; Parsons et al. 1996), and that topography enhances the tidal motion (tidal rectification) through bottom friction and planetary vorticity (Loder 1980; Vinje et al. 1989; McClimans & Nilsen 1993; Kowalik & Proshutinsky 1995; Padman 1995).

The Polar Front occurs at the junction of Atlantic Water and Arctic Surface Water, and nearly coincides with the slope of the bottom topography in Hopendypet (Harris et al. 1998). A mixture of these water masses forms another type of water mass which Loeng (1991) calls Barents Sea Water (BSW), and Pfirman et al. (1994) call Atlantic derived water. The BSW of Loeng (1991) is characterized by temperatures between -1.5 °C and 2 °C and salinities between 34.7 and 35.0. Pfirman et al. (1994) use the limits of -2 °C < T < 0 °C and 34.75 < S < 34.95 to characterize the Atlantic derived water. In the Arctic Ocean and in the Norwegian-Greenland Sea these watermasses have been called Arctic intermediate water (Swift 1986).

As we see, different authors use different names and acronyms of water masses that have equal or close to equal water mass characteristics. Different authors have also extended or reduced the intervals of temperature and salinity, which defines the different water masses. Recent publications such as Blindheim et al. (2000) also provide evidence that the regional climate changes the properties of the different water masses, and the structure of distribution of these water masses, on scales of decades and centuries. They found that the upper layer of the Norwegian Sea
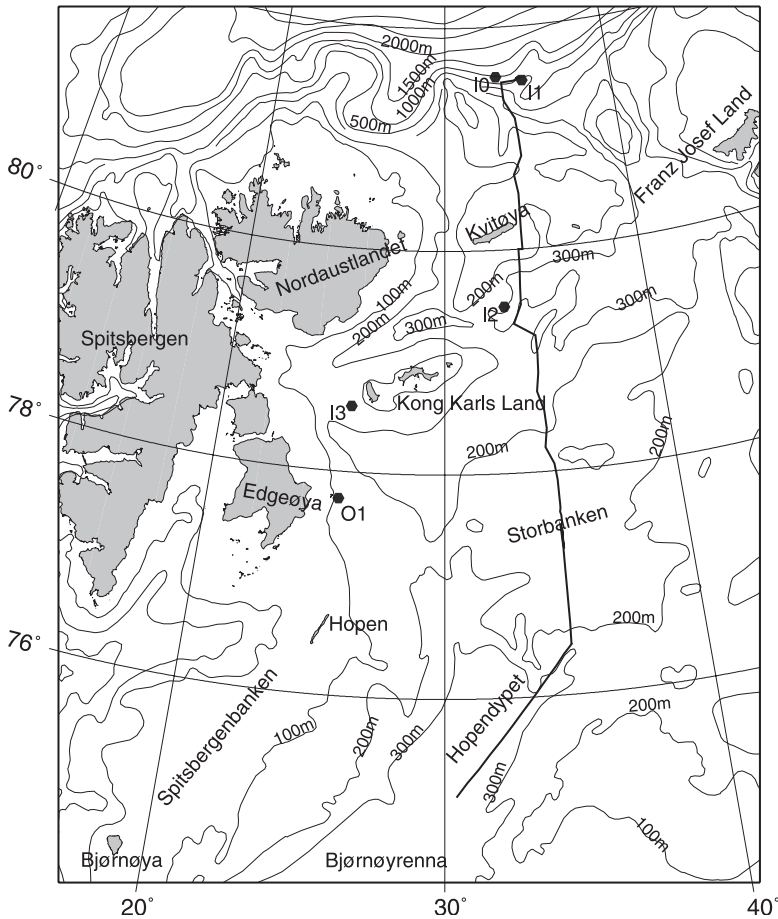
Fig. 1. Map of the north-west Barents Sea indicating the transect (thick north—south line) and five drifting stations (I0, I1, I2, I3 and O1) discussed in this paper. Also shown are contour lines for the 100 m, 200 m and 300 m isobaths. The contour lines at the shelf break north of Kvitøya are not consistent with the echo-sounding depth at the drift stations I0 and I1. Depth information from *The general bathymetric chart of the oceans* (British Oceanographic Data Centre 1997).

has become cooler and fresher since the 1960s. Østerhus et al. (1996) have found that the deep water in the Norwegian Sea has become warmer. The concept of change in the water mass characteristics occuring with a climatic change has been adopted by Pfirman et al. (1994), where they divide the Atlantic derived water mass in two parts based on the different years of origin, i.e. different "vintages". The part of the NAC that continues northwards along the west coast of Spitsbergen meets the Arctic water north of the Svalbard Archipelago, submerges under it, and follows the bathymetry eastwards into the Arctic Ocean. On the north-east side of Nordaustlandet, some part of this Atlantic water turns south as it follows the bathymetry between Nordaustlandet and Kvitøya and between Kvitøya and Franz Josef Land. This water mass would be, according to Pfirman et al. (1994), about two years older than the water mass of Atlantic origin coming

from the south through Bjørnøyrenna into the western Barents Sea. Due to the interannual variation in the NAC, and the interannual and seasonal variations of the climate in the region, these two water masses (with the same origin) would have different properties of T and S. To distinguish them, Pfirman et al. (1994) use the terms Northern Barents Sea Atlantic-derived Water (NBAW) and Southern Barents Sea Atlantic-derived Water (SBAW). For the years 1981 and 1982, the NBAW was generally less saline than the SBAW. Steele et al. (1995) show that these water masses of Atlantic origin are transformed by atmospheric cooling and ice melting into a water mass type with properties identical to the lower halocline water of the Arctic Ocean. Their observations from the Coordinated Eastern Arctic Experiment (CEAREX) in October–December 1988 show little evidence of salinization of the surface shelf waters by sea ice formation. They

Hydrography in the north-western Barents Sea

cannot provide any evidence of Arctic Ocean deep water formation, and they assume that the measurements were taken too early in winter to detect any salinization.

The purpose of this paper is, first, to give a description of the hydrographic situation the northern Barents Sea in July–August 1996, based on the collected CTD data set, and to compare this with former investigations. Second, the paper aims to establish and document the horizontal scales of variation to provide a basis or a framework for further studies of the general circulation and mixing processes in the area.

Instruments and methods

The measurement programme consisted of CTD profiles, continuous shipboard ADCP sampling, and dissolved organic carbon (DOC) samples. The analysis and discussion in this paper will concentrate on the CTD profiles which were taken along a generally northward transect and during time series stations where the ship was anchored to a drifting ice floe while samples were taken regularly (Fig. 1). As illustrated in Fig. 1, the northward transect consisted of two segments, one that went in a north-eastward direction from Hopendypet to Storbanken, and a longer one that extended more directly northward from Storbanken to the shelf break in the Arctic Ocean. The north-eastward segment from Hopendypet to Storbanken was about 147 km long; 11 CTD casts wer made along this segment of the transect. The length of the northward segment was 566 km and included 39 CTD profiles.

The fundamental basis for the choice of location was different type of ice biotops/ice conditions: very close or close drift ice (I0, I1); open or very open drift ice (I2, I3); and open water (O1).

The locations of I0 and I1 are very close to one another; they were chosen because of the different topography. Information about the drift of the different stations is given in Table 1.

The equipment used was a Neil Brown IIIB CTD together with a General Oceanics Rosette sampler. The CTD was calibrated before the cruise, and the salinity estimations were compared with analysis of water samples on board during the cruise. A regression analysis of the the water samples vs. the CTD measurements gave us a linear relation between the two different salinities:

$$S_{Bottle} = 0.9981 \, S_{CTD} + 0.05134 \quad (1)$$

All the salinities measured by the CTD were corrected according to Equation (1). Further details concerning Equation (1) can be found in Løyning & Budgell (1996).

To be able to discuss horizontal variations of the hydrographical conditions, we need to estimate a typical length and a time scale from the observations. One possibility for the length scale is the Rossby radius of deformation, the minimum length scale typifying a mesoscale process, which dominates spatial scales between the basinwide gyres in the world oceans and small-scale features such as internal waves. For scales that are small compared with the Rossby radius of deformation, rotational effects on the currents are small. For processes with scales that are of the same size or larger than the Rossby radius of deformation, rotational effect must be considered (Muench 1990). The mesoscale phenomena in the ocean can have both baroclinic and barotropic origins, where the baroclinic effects are related to the the density variations and are therefore depth dependent, whereas the barotropic part is independent of depth. Examples of features dominated by baroclinic behaviour are local fronts and

Table 1. The average values of the drift at five drift stations in the north-western Barents Sea: average position; total drift period; distance in km between start and end positions; overall drift direction in compass degrees; average time interval; and distance and speed between the CTD stations.

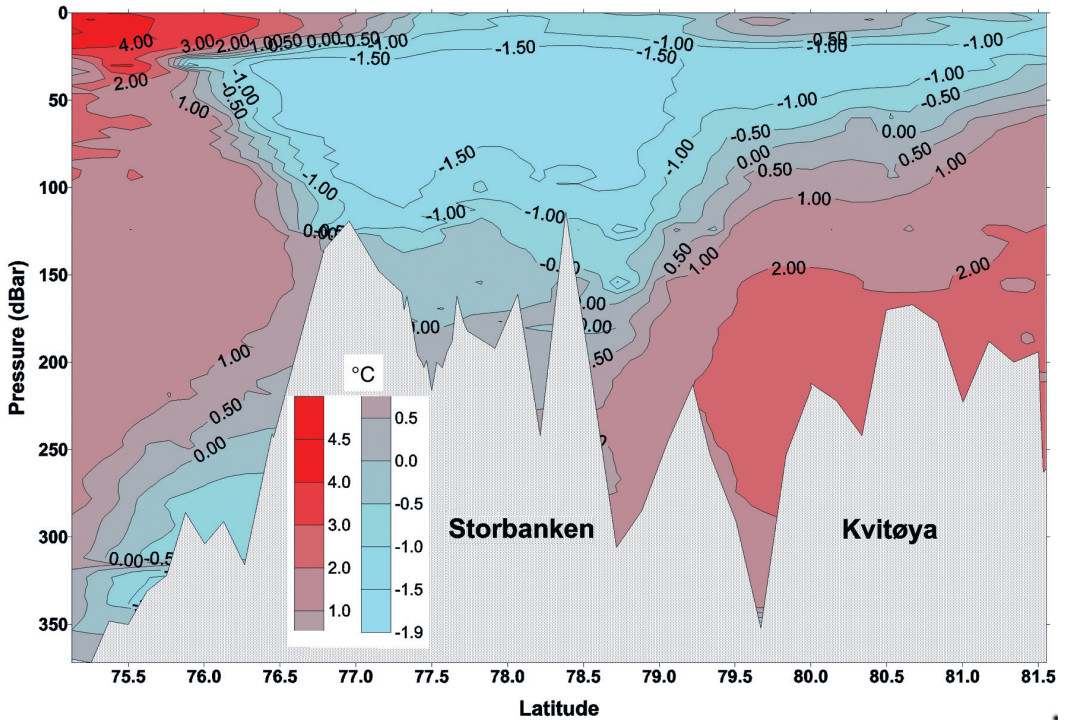| Station	Position		Total drift			Intervals		
	lat. N	long. E	hours	km	direction	hours	km	m/s
I0	81.55	33.08	39.7	15.0	147° SE	4.9	2.7	0.15
I1	81.51	34.68	89.9	21.0	203° SW	2.4	0.8	0.10
I2	79.49	32.91	31.7	17.1	83° E	4.0	3.3	0.25
I3	78.59	25.80	26.0	13.9	5° N	3.3	2.3	0.18
O1	77.76	25.52	12.9	4.8	126° SE	4.3	2.7	0.17

Fig. 2. Contour lines of potential temperature along the transect. The 0 ºC degree contour line is slightly thicker than the others. Warm water is red; cold water is blue (see key).
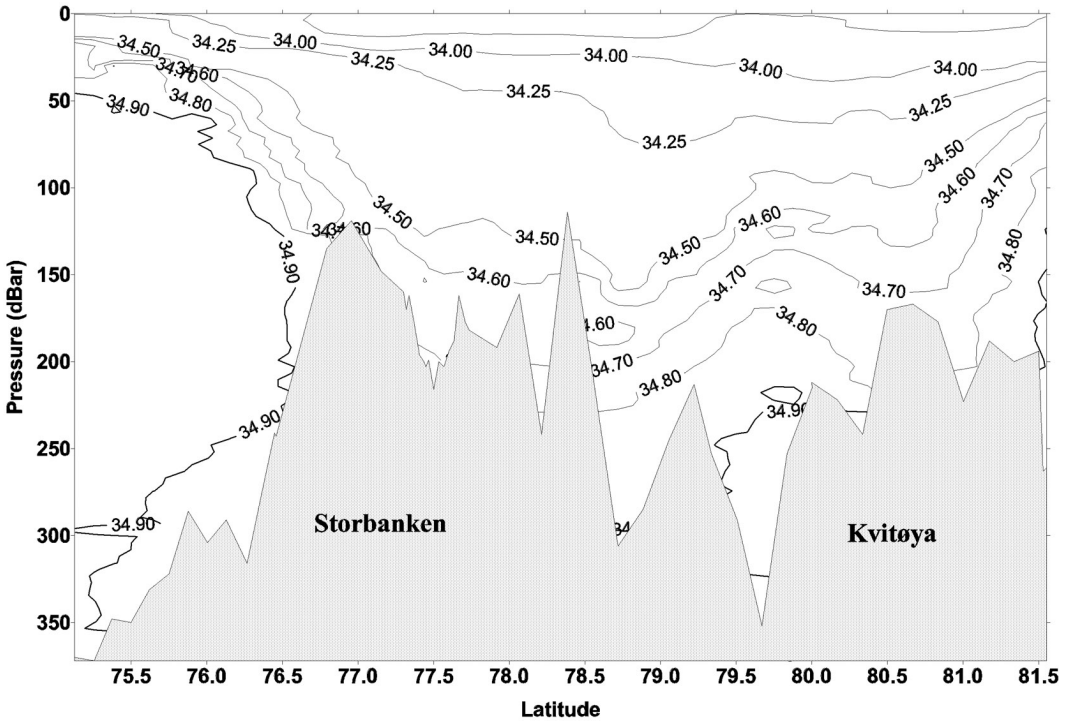

Fig. 3. Contour lines of salinity along the transect. The 34.9 contour line is slightly thicker than the others.

Hydrography in the north-western Barents Sea

Fig. 4. θS diagram of all the CTD profiles from the transect. Green stars are observations in Hopendypet, south of Storbanken (south of 76.5° N). Blue crosses are observations at Storbanken, from 76.5° N to 79° N. Red dots indicate the observations north of Storbanken (north of 79° N).
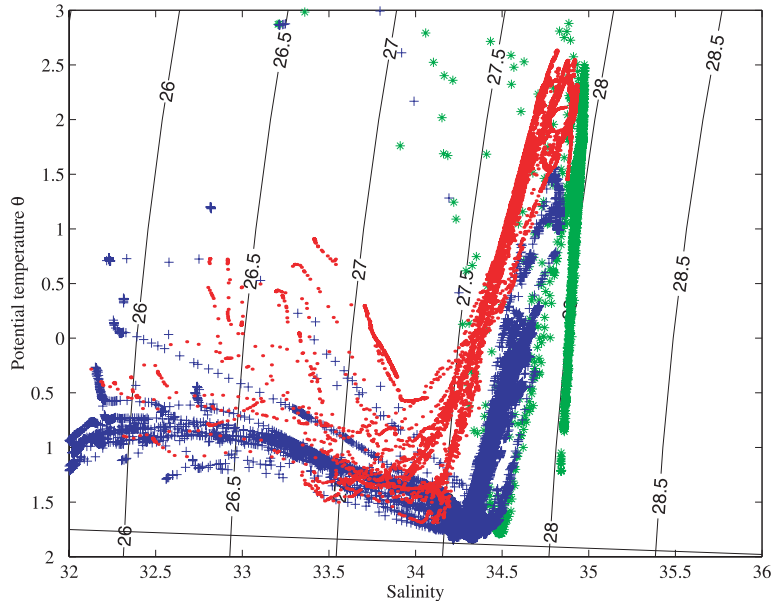
eddies in a highly stratified environment close to the surface, typical along melting ice edges. The first mode of the Rossby radius (Table 2) will therefore be an appropriate cross-frontal length scale. Eddies and fronts may also have barotropic behaviour, i.e. the currents linked to the features will extend to the bottom of the sea. The Rossby radius is defined as

$$a_n = c_n/f, \; n = 1,2,... \qquad (2)$$

where c_n is a characteristic speed of a baroclinic feature for a mode n, and $f = 2\,\Omega \sin \varphi$ is the Coriolis parameter. (Ω is the angular velocity of the Earth's rotation, and φ is the latitude.) The values of c_n are found using the theory of normal modes, solving an eigenvalue problem (Haberman 1983; Emery & Thomson 1998). The basic assumptions of this theory is that the horizontal spatial scales are much larger than the vertical scales, and that the ocean depth is constant. For a description and discussion of the hydrographic conditions, the first assumption is valid, since the depth in the area is less than 400 m. The latter assumption is not valid in this area since there are indiciations that topography may have a larger influence on the circulation, but as a crude approximation it may provide some useful information. The barotropic Rossby radius of deformation is given by the Equation (2), replacing c_n with $c = \sqrt{gH}$, where g is the acceleration due to gravity and

H is the average depth in the area (i.e. depth of the stations). In the formulation of the eigenvalue problem, the buoyancy frequency N is included, defined by:

$$N^2 = -\frac{g}{\rho_m}\frac{\partial\rho}{\partial z} + \frac{g^2}{C} \simeq -\frac{g}{\rho_m}\frac{\partial\sigma_t}{\partial z} \qquad (3)$$

where ρ_m is a reference density (average of the water column), $\partial\rho/\partial z$ is the change of the density with depth, g is the acceleration due to gravity, C is the speed of sound in sea water and $\sigma_t = \rho(T,S,0)-1000$. The approximation in Equation (3) is justified in the upper parts of the ocean (upper 1000 m) where compressibility can be neglected. N may give us the typical time scale for dynamical features in the area, and is linked to the spatial scale through the estimations of c_n used in Equation (2). The Rossby radius is estimated for each CTD profile at each drift station, assuming a constant depth (the depth of the profile) and using a mean value of the buoyancy frequency N from each profile.

Presenting our observations as contour lines, we have used the method of Krieging to convert our irregularly spaced data set into a gridded data set. We might have chosen other methods, but according to Davis (1986) there is no formal statistical theory that allows us to predict, on theoretical grounds alone, which contouring procedure might be superior. The choice is therefore merely

based on appearance, although the appearance of a contour map is not a reliable guide to how well the underlying mathematical model represents the original control points. The spacing between gridpoints has been chosen to be close to the average distance between CTD stations.

Hydrography

The numbers presented in Table 2 are averages of all the estimated Rossby radii at each drift station, estimated from Equation (2). Average depth of the CTD profiles at the different drift stations has been used to estimate the barotropic Rossby radius.

Figure 2 shows the temperature field of the section. There is a cold water mass on top of Storbanken, with a core temperature less than –1 °C. On both sides of this cold water, there are warmer water masses which lie under the cold water at the northern side, but at the same depths on the southern side. The warmest water $\theta > 4$ °C can be found at the surface south of 76° N, and we see that the temperature decreases northwards over a distance of about two degrees latitude, similar to about 200 km. The vertical gradients are more clearly defined on the southern side of Storbanken than on the northern side. South of Storbanken, at the slope below 250 dBar there is also a cold water mass.

In Fig. 3 we see the contour lines of salinity. The water mass with a salinity value of 34.9 and higher can be found south of Storbanken and in the deeper parts of the section. Salinities equal to or above 35 were not found. South of Storbanken there is a water mass with salinities above 34.9 and there is a clearly defined gradient dividing this salt water mass from the fresher water mass ($S < 34.5$) further north. The gradient stretches downwards from the surface in the southern end to the sea bottom at Storbanken.

Table 2. The barotropic Rossby radius and the first four baroclinic Rossby radii.

| Drift stations | Rossby radii (km) | | | | |
| | Barotropic mode | Baroclinic | | | |
		mode 1	mode 2	mode 3	mode 4
I0	449.7	3.5	1.8	1.2	0.9
I1	308.6	3.0	1.5	1.0	0.7
I2	367.9	3.4	2.0	1.2	0.9
I3	252.5	3.1	1.3	0.9	0.7
O1	264.2	2.1	1.2	0.7	0.6

Figure 4 shows a θS diagram for the sections from Hopendypet to the shelf break of the Arctic Ocean. The southernmost water mass (in Hopendypet, south of Storbanken) shows very little freshening; this water mass reaches σ_θ values higher than 28.0 kg/m^3, and temperatures down to –1 °C. The water mass from above Storbanken (76.5° N to 79° N) is slightly fresher, indicating local mixing processes with fresher and colder water. The modification of the northernmost water mass (north of 79° N) is also dominated by cooling, but freshening through mixing is larger for this water mass than for the others.

Among the nine CTD casts at the drift station I0, the deepest station was at 800 m depth and the shallowest at 180 m. Figure 5 shows a θS diagram from these stations. The warmest water is found at 100 dbar with $\theta > 2.5$ °C. The salinity at this level is $S > 34.9$. The most saline water is found much deeper, at 400 dbar, where $S > 35$ and where the temperature is slightly lower ($\theta \approx 2.3$ °C). A nearly straight line can be drawn from the coldest and freshest water at the surface ($\theta \approx -1.5$ °C, $S < 32.5$) to the warm and more saline deeper parts ($\theta > 2$ °C, $S > 34.5$). The straight mixing line indicates that there are local mixing processes present.

Figure 6 shows potential temperature vs. salinity from the CTD cast at the drift station I1 at the continental shelf north-east of Spitsbergen. During the measurements at the station, the upper 50 m had a temperature variation of nearly one degree. The water mass becomes more homogeneous closer to the bottom. The temperature increases from around –1 °C at the surface to above 2 °C at the bottom. Compared to the θS diagram from station I0 (Fig. 5) we can see that the surface has become slightly warmer (0.5 °C), but the the upper 50 m has been cooled.

The θS diagram at the drift station I2 (Fig. 7) shows a very different picture from Figs. 5 and 6, at least for the upper parts. Here the temperature increases at the first 10 m from 0 °C to 1 °C, then it drops nearly two degrees, and finally the temperature increases towards the bottom, like what we find in Figs. 5 and 6. This could be explained by a longer exposure of the surface to the sun and thereby heating of the upper parts. The slightly increased salinity could be attributed to the mixing of subsurface layers into the surface layer.

South-west of Kong Karls Land, the θS diagram of drifting station I3 (Fig. 8) shows a pic-
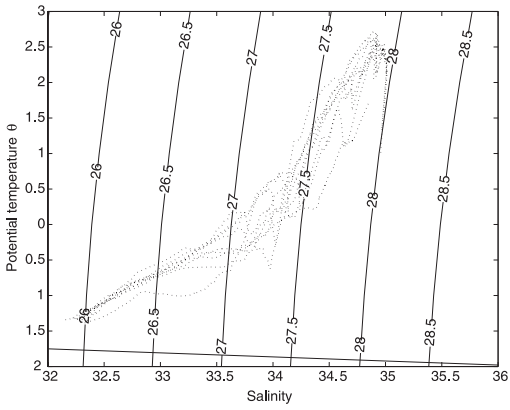
Fig. 5. Potential temperature vs. salinity at drifting station I0.
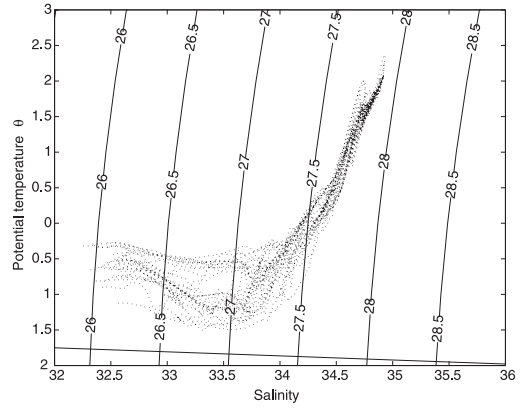The reference pressure is 0 dbar.

Fig. 6. Potential temperature vs. salinity at drifting station I1.
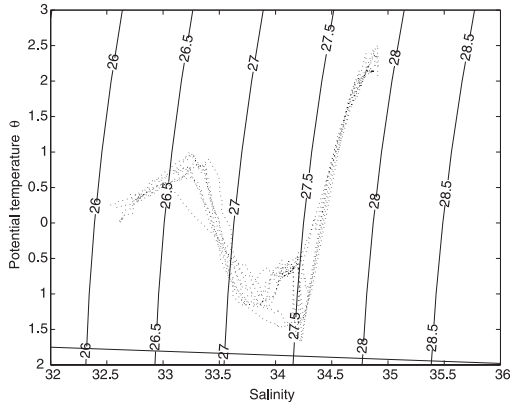The reference pressure is 0 dbar.

Fig. 7. Potential temperature vs. salinity at drifting station I2.
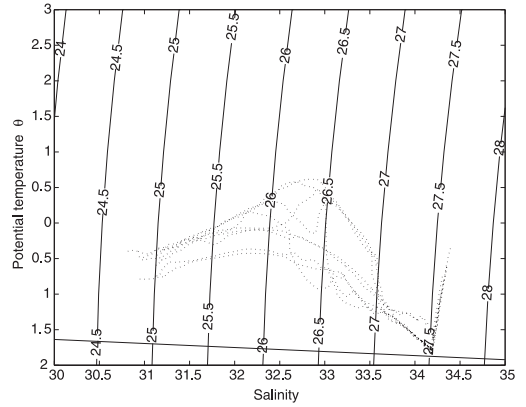The reference pressure is 0 dbar.

Fig. 8. Potential temperature vs. salinity at drifting station I3.
The reference pressure is 0 dbar.

ture different than from the other stations further
north. Here the surface layers are colder than at
station I2 north of Kong Karls Land. Further-
more, there is a larger variation in the subsurface
layers and very a homogeneous water mass at the
lower parts, with a very sharp temperature mini-
mum below –1.5 °C.

The four CTD casts of the open ocean drift sta-
tion O1 presented in Fig. 9 as a θS diagram, reveal
a temperature minimum like the station I3 (Fig.
8), but with a much warmer surface layer. The
straight line from the temperature maximum to
the temperature minimum indicates local verti-
cal mixing, and no intrusion or advection of water
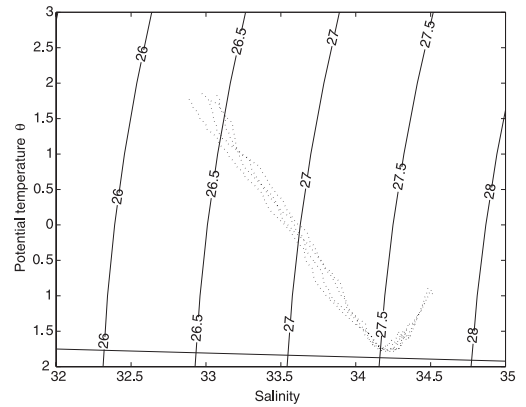masses with other θS properties.

Fig. 9. Potential temperature vs. salinity at drifting station O1.
The reference pressure is 0 dbar.

Discussion

A general remark can be said about using average values when the Rossby radius is calculated, especially on using an average of the buoyancy frequency N. Normally, the regions of strong gradients and stable hydrographic conditions and therefore high values of N are to be found in the upper parts of the water column, with weaker stratification and lower values of N in the rest of the water column. The difference can be one order of magnitude. The region of weak stratification is usually much larger than the upper parts, and the average value of N will be biased by this region. Smaller values of N imply smaller values of the Rossby radius of deformation. As a consequence, the Rossby radius of deformation in the upper mixed layer would be larger than the values presented in Table 2 and smaller in the water masses below the pycnocline. However, these crude estimates provide some information about the synoptic scales of the ocean in the investigation field and the influence of the Earth's rotation, i.e. the spatial and time scales of the processes that dominate the variations in the properties and state of the ocean, such as the density field and velocity distribution. Given all these assumptions, together with those in the section of instruments and methods, we may suggest that rotational effects should be considered when variations on a larger scale than 3 km are to be explained. This length scale should be considered when future field programmes are planned.

As explained earlier, Northern Barents Sea Atlantic derived Water (NBAW) and Southern Barents Sea Atlantic derived Water (SBAW) have the same Atlantic origin, but they originate from different years. NBAW and SBAW may be seen in Figs. 2 and Fig. 3, NBAW on the righthand side of the figures and SBAW on the left. This is most clear in Fig. 2. The difference between the two water masses may also be seen in Fig. 4. The different mixing lines of these water masses are distinct, and we see that the SBAW is saltier than the NBAW, as also observed by Pfirman et al. (1994). We can also see in Fig. 4 that the mixing line of SBAW is nearly vertical and therefore little freshening by melting or salinization by freezing has occured compared to the other mixing lines. The modification of the SBAW therefore is mostly due to cooling at the surface. This strong cooling of a relative salt water mass produce the densest water found in this data set.

In Fig. 2 we can see that the coldest water mass can be found above Storbanken and northwards, and along the southern slope of Storbanken. From Fig. 4 we can see that the water masses above Storbanken have been modified both by salinization through freezing of sea water and by melting of sea ice. Figure 4 agrees very well with the observations of Aagaard, Coachman et al. (1981) in their general explanation of the maintenance of the cold halocline layer in the Arctic Ocean. They propose that the salinization of water masses on the shelves around the Arctic Ocean and then convection and advection into the Arctic Ocean may contribute to the maintenance of the halocline. They have also suggested that the effect of temperature on compression where cold water is more compressible than warmer water, i.e. the thermobaric effect, may promote deep convection (Aagaard, Swift et al. 1985; Aagaard & Carmack 1994). Løyning & Weber (1997) found a necessary criterion involving the temperature and salinity gradients to get thermobaric enhanced convection. The thermobaric effect upon mixing and convection may therefore be found on the shallow shelves around the Arctic Ocean, as well as in the deep waters. Some of these suggested processes may explain the cold and salt volume of water along the southern slope of Storbanken, as shown in Fig. 2. This water mass has probably been formed on Storbanken, and is then sinking into Hopendypet and Bjørnøyrenna and into the Norwegian and Greenland seas.

Another mechanism proposed by Aagaard, Coachman et al. (1981) is the cooling and freshening of Atlantic Water (AW: S > 35, T > 1 °C) in the vicinity of the continental shelves around the Arctic Ocean. Here AW is supposed to be forced to the surface by upwelling, where it is cooled by the atmosphere and melting sea ice, and thereby also becomes fresher. Evidence of such upwelling has been found on the shelf of the Alaskan Beaufort Sea, where it may happen regularly (Aagaard, Coachman et al. 1981). From Figs. 2 and 3 we cannot find signs of upwelling of Atlantic Water or Atlantic derived water (NBAW) in the northern region, close to the shelf break. However, the geographical division of water masses and mixing lines in Fig. 4 shows that the NBAW may be transformed to a water mass with the same characteristics as the cold halocline layer of the Arctic Ocean if we follow the definitions of Steele et al. (1995) and Aagaard, Coachman et al. (1981): CHW: 34 < S < 34.5 and θ < -0.5 °C. Compared

to the other geographic regions, the NBAW contributes less to the Cold Halocline Water (CHW) mass. This picture may also be confirmed by the results from the two northernmost drift stations. The θS diagrams from station I0 and I1 (Figs. 5, 6), close to the shelf break to the Arctic Ocean (Fig. 1), show mixing lines that pass outside or barely touch into the characteristics of CHW.

The concept of upwelling may be used to explain the warmer layer close to the bottom at Storbanken, as depicted in Fig. 2. The layer close to the bottom is one half of a degree warmer than the water mass above it. An explanation of the upwelling may be given in terms of tidal dynamics. In a study by Kowalik & Proshutinsky (1995) concerning topographic enhancement of tidal motion, the authors discuss several effects of interaction between bottom topography gradients and tidal motion at the shallow banks in the western Barents Sea, i.e. south-west of the investigation area. They find that residual motion induced by tides around Bjørnøya (Bear Island) and Spitsbergenbanken clearly depicts circular eddies trapped around topographic features. With reference to the literature (Zimmerman 1978; Robinson 1981; Pingree & Maddock 1985), they explain that these circular eddies are related to the oscillating velocity field, i.e. vorticing is generated by tidal motion and friction over sloping topography. They also find good agreement between their observations of residual circular currents and rotation around Bjørnøya and over Spitsbergenbanken and general patterns generated from simpler models.

Kowalik & Proshutinsky (1995) also discuss tide induced vertical residual currents in the neighbourhood of Bjørnøya. Strong horizontal tidal motion over shallow and variable topography ought to be associated with strong vertical motion. Their calculation of vertical velocities from the equation of continuity results in vertical velocities on the order of $1.0 \cdot 10^{-3}$ cm/s. The results from their numerical tidal model show that Bjørnøya is surrounded by horizontal alternating chimneys of upwelling and downwelling. This residual upwelling and downwelling can couple with the tidal mixing along the Bjørnøya shelf and Spitsbergenbanken and bring Atlantic water onto the shelves and into the surface layer. We may assume that these processes also occur further north in the Barents Sea, around Storbanken, and on the shallow topography around the islands of Kong Karls Land and Kvitøya. The tide induced

horizontal and vertical currents over the banks may be the reason that we observe half a degree warmer water on the Storbanken close to the bottom in Fig. 2. Pfirman et al. (1994) conclude that Atlantic water from Hopendypet also crosses the polar front, flowing northwards over a sill between Storbanken and Spitsbergenbanken further south (Fig. 1). Harris et al. (1998) oppose this conclusion and state that they are not aware of a dynamical mechanism whereby Atlantic water can flow through the polar front region and over this sill. We suggest that although Atlantic water may not flow over the sill, it seems that SBAW may do so, possibly forced by tidal interactions with topography.

Figure 7 shows the temperature and salinity charcteristics from drift station I2, located south of Kvitøya. Here the processes of cooling and freshening produce a mixing line that points directly to the definition of CHW. This location is also in the trench system that has an outlet to the Arctic Ocean between Kvitøya and Franz Josef Land. CHW from this region may contribute to the cold halocline layer in the Arctic Ocean as proposed by Aagaard, Coachman et al. (1981).

The drift station I3 is located close to the islands of Kong Karls Land, and Fig. 8 reveals a very sharp discontinuity in the region of the CHW characteristics, and strongly defined mixing lines, both in directions of cooling and of salinization. The observations further south at the drift station in open waters, O1 (Fig. 9), shows a smoother change of properties. This difference may be explained by different dynamic regimes. The location of the drift station is close to the outlet of Hinlopen Stredet, the strait or channel between Nordaustlandet and western Spitsbergen (Fig. 1). Water channelled through this strait may have been discharged a short time before our measurements, with little or no time for diffusive and mixing prosesess to smooth out the gradients. The open water drift station (O1) is closer to the shore and eddies generated from the coast may trap water masses for a longer time. Our drift pattern at this station may indicate a possible eddy.

Steele & Morison (1993) note that their observations between 81.6° N and 82.4° N fail to support the theory of Aagaard, Coachman et al. (1981) that halocline water is formed by an ice growth mechanism, and that this halocline water formation may take place at the shelf of the northern Barents Sea. They conclude that if this is so, the CEAREX data indicate that these processes

would occur later in winter or at another part of the shelf, where they had no data. Steele et al. (1995) discuss the halocline water formation in the Barents Sea, using data collected during the CEAREX, drifting from north to south through the Barents Sea. They conclude that some halocline may form north of the marginal ice zone (MIZ), defined as the zone between open water and pack ice. The mechanism for this formation is by entrainment of Atlantic Water into the surface layer, and subsequent modification due largely to ice melting. Steele et al. (1995) found little evidence of halocline formation by salinization of surface water during ice growth.

This study's findings (Fig. 4) indicate that CHW may be formed by modification of Atlantic derived water (NBAW or SBAW) through cooling and ice melting, as mentioned by Steele et al. (1995). The mixing lines for the waters above Storbanken also indicate that CHW may have been formed above Storbanken through a salinization process during ice growth, which Steele et al. (1995) did not find in their observations.

Transformation of water mass with an Atlantic origin by melting and cooling north-east of Spitsbergen and north-west of Franz Josef Land in the Nansen Basin is also reported by Schauer et al. (1997). They found intrusions of colder and fresher water between 200 and 500 m that apparently come from the shelves of the northern Barents Sea. They concluded that shelf bottom water that drains from the Barents Sea north into the western Nansen Basin can, even though small in volume, significantly modify the core properties of what they call the Fram Strait Branch Water (which we have called NBAW). They further concluded that the intrusion's influence on the density distribution can influence the internal dynamics of the regional eastward slope current. Our observations from ice drift station I0 is in close agreement with the observations presented by Schauer et al. (1997) and Steele & Morison (1993).

Although neither the transect described here nor the transect analysed by Steele et al. (1995) are synoptic, they are quite similar, with a cold and fresh layer above Storbanken, and warmer and saltier water further north. This may support a hypothesis that the water mass above Storbanken is stationary, surrounded by warmer and saltier water mass, SBAW in the south and NBAW in the north. If the hypothesis of tide induced circulation around Storbanken is correct, the center of this gyre would be stationary, which also may

lead one to conclude that the cold and fresh water mass stays put above Storbanken.

During autumn and winter this water mass is modified by cooling and salinization through sea ice formation at the surface. Atlantic water may be entrained and mixed into this water mass from the under side through tidal dynamics as explained above. These processes may transform the water masses on Storbanken into CHW and CDW, which may sink down from Storbanken to the south into the Bjørnøyrenna–Hopendypet region, to the north into the channel between Franz Josef Land and Kvitøya.

Summary and conclusion

This paper has presented a general picture of the hydrographic situation in the northern Barents Sea in the summer of 1996, from Hopendypet at 75.1° N to the shelf break of the Polar Ocean at 81.6° N. Due to special weather and ice conditions, the ice retreated as we moved northwards along the 35° E. Estimations of the scales of variation of the hydrographic fields are presented, showing that the first baroclinic mode of the Rossby radius of deformation is around 3 km in this area at this particular time of year.

Warmer Atlantic derived water mass from the south (SBAW) and from the north (NBAW) have different properties, due to different years of origin, and meet in the troughs and channels around Storbanken and on Storbanken close to the bottom. This paper suggests the tidal rectification as the energy source for the transport of SBAW and NBAW above and across the sills and banks. Therefore, when planning future field programmes in this region, the scales of variation of topography and the first mode of the Rossby radius should be considered.

Different mixing lines of these different water masses show that the SBAW is the most likely source for cold halocline water and cold deep water in this region of the Barents Sea, together with the coldest water mass above Storbanken. A cold water mass is also found on the southern slope of Storbanken, under the SBAW, in the Hopendypet–Bjørnøyrenna trench system, which leads into the Nordic Seas. Such cold and dense water mass is not found on the northern side of Storbanken. These observations may support a hypothesis that the CHW is produced in regions around Storbanken in the western Barents Sea,

and not at the shelf regions further north and closer to the continental shelf break.

References

Aagaard, K. & Carmack, E. C. 1994: The Arctic Ocean and climate: a perspective. In O. Johannesen et al. (eds.): *The polar oceans and their role in shaping the global environment. Geophys. Monogr. 85*, 199–209. Washington, D.C.: AGU.

Aagaard, K., Coachman, L. K. & Carmack, E. 1981: On the halocline of the Arctic Ocean. *Deep-Sea Res. 28*, 529-545.

Aagaard, K., Swift, J. H., & Carmack, E. C. 1985: Thermohaline circulation in the Arctic Mediterranean seas. *J. Geophys. Res. 90(C2)*, 4833–4846.

Blindheim, J., Borovkov, V., Hansen, B., Malmberg, S.-A., Turrel, W. R., & Østerhus, S. 2000: Upper layer cooling and freshening in the Norwegian Sea in relation to atmospheric forcing. *Deep-Sea Res. Part I 47*, 655–680.

British Oceanographic Data Centre 1997: *The general bathymetric chart of the oceans (GEBCO 97)*. CD-ROM. Birkenhead, UK: BODC.

Davis, J. C. 1986: *Statistics and data analysis in geology.* Second edition. New York: John Wiley & Sons.

Emery, W. J. & Thomson, R. E. 1998: *Data analysis methods in physical oceanography.* Oxford: Pergamon.

Gawarkiewicz, G. G. & Plueddemann, A. J. 1995: Topographic control of thermohaline frontal structure in the Barents Sea Polar Front on the south flank of the Spitsbergen Bank. *J. Geophys. Res. 100(C3)*, 4509–4524.

Haberman, R. 1983: *Elementary applied partial differential equations.* Englewood Cliffs, NJ: Prentice-Hall.

Harris, C. L., Plueddemann, A. J. & Gawarkiewicz, G. G. 1998: Water mass distribution and polar front structure in the western Barents Sea. *J. Geophys. Res. 103(C2)*, 2905–2917.

Helland-Hansen, B. & Nansen, F. 1909: *The Norwegian Sea: its physical oceanography based upon Norwegian researches 1900–1904. Rep. Nor. Fish. Mar. Invest. 2(2).* Kristiania (Olso): Mallingske Book Publ.

Johansen, Ø., Mathisen, J. P. & Steinbakke, P. 1988: *Environmental data collection in the Barents Sea. Rep. OCE 88059.* Trondheim: Oceanor.

Kowalik, Z. & Proshutinsky, A. Y. 1995: Topographic enhancement of tidal motion in the western Barents Sea. *J. Geophys. Res. 100(C2)*, 2613–2637.

Loder, J. W. 1980: Topographic rectification of tidal currents on the sides of Georges Bank. *J. Phys. Oceanogr. 10*, 1399–1416.

Loeng, H. 1990: *Current measurements southeast of Sentralbanken in the Barents Sea. Institute of Marine Research Rep. FO 9002.* Bergen.

Loeng, H. 1991: Features of the physical oceanographic conditions of the Barents Sea. *Polar Res. 10*, 5–18.

Løyning, T. B. & Budgell, W. P. 1996: *Physical oceanography data report from the ICEBAR cruise 1996. Nor. Polarinst. Rapp.ser. 95.* Oslo: Norwegian Polar Institute.

Løyning, T. B. & Weber, J. E. 1997: Thermobaric effects on buoyancy-driven convection in cold seawater. *J. Geophys. Res. 102(C13)*, 27875–27885.

McClimans, T. A. & Nilsen, J. H. 1993: Laboratory simulation of the ocean currents in the Barents Sea. *Dyn. Atmos. Oceans 19*, 3–25.

Muench, R. D. 1990: Review of mesoscale phenomena in the polar oceans. In W. O. Smith, Jr. (ed.): *Polar oceanography. Part A, Physical Science.* Pp. 223–285. San Diego: Academic Press.

Østerhus, S., Turrel, W. R., Hansen, B., Blindheim, J. & Van Bennekom, A. J. 1996: Changes in the Norwegian Sea Deep Water. Document presented at International Council for the Exploration of the Sea Council Meeting: ICES Annual Science Conference, Reykjavík, 27 September–1 October 1996.

Padman, L. 1995: Small-scale physical processes in the Arctic Ocean. In W. O. Smith, Jr. & J. M. Grebmeier (eds.): *Arctic oceanography: marginal ice zones and continental shelves. Coast. Estuar. Stud. 49*, 97–129.

Parsons, A. R., Bourke, R. H., Muench, R. D., Chiu, C.-S., Lynch, J. F., Miller, J. H., Plueddemann, A. J. & Pawlowicz, R. 1996: The Barents Sea Polar Front in summer. *J. Geophys. Res. 101(C6)*, 14201–14221.

Pfirman, S. L., Bauch, D. & Gammelsrød, T. 1994: The northern Barents Sea: water mass distribution and modification. In O. Johannesen et al. (eds.): *The polar oceans and their role in shaping the global environment. Geophys. Monogr. 85*, 77–94. Washington, D.C.: AGU.

Pingree, R. D. & Maddock, L. 1985: Rotary currents and residual circulation around banks and islands. *Deep-Sea Res., Part A, 32*, 929–947.

Robinson, I. S. 1981: Tidal vorticity and residual circulation. *Deep-Sea Res., Part A, 28*, 195–212.

Rudels, B. 1987: *On the mass balance of the Polar Ocean, with special emphasis on the Fram Strait. Nor. Polarinst. Skr. 188.* Oslo: Norwegian Polar Institute.

Schauer, U., Muench, R. D., Rudels, B. & Timokhov, L. 1997: Impact of eastern Arctic shelf waters on the Nansen Basin intermediate layers. *J. Geophys. Res. 102(C2)*, 3371–3382.

Steele, M. & Morison, J. H. 1993: Hydrography and vertical fluxes of heat and salt northeast of Svalbard in autumn. *J. Geophys. Res. 98(C6)*, 10013–10024.

Steele, M., Morison, J. H., & Curtin, T. B. 1995: Halocline water formation in the Barents Sea. *J. Geophys. Res. 100(C1)*, 881–894.

Swift, J. H. 1986: Arctic waters. In B. G. Hurdle (ed.): *The Nordic seas.* Pp. 129–153. New York: Springer.

Vinje, T., Jensen, H., Johnsen, Å. S., Løset, S., Hamran, S.-E., Løvaas, S. M. & Erlingsson, B. 1989: *IDAP-89 R/V Lance Deployment. Vol. 2. Field observations and analysis.* Oslo / Trondheim: Norwegian Polar Inst. / SINTEF NHL.

Zimmerman, J. T. F. 1978: Topographic generation of residual circulation by oscillatory (tidal) currents. *Geophys. Astrophys. Fluid Dyn. 11*, 35–47.